

1 **A GIS-based model of outdoor thermal comfort: Case study for Zurich**

2

3 Jonas Hess

4 Institute for Transport Planning and Systems, ETH Zürich

5 CH-8093 Zurich

6 ORCID: 0000-0003-0857-4378

7 johess@ethz.ch

8

9 Adrian Meister

10 Institute for Transport Planning and Systems, ETH Zürich

11 CH-8093 Zurich

12 ORCID: 0000-0002-3350-9044

13 adrian.meister@ivt.baug.ethz.ch

14

15 Valentin Melnikov

16 Institute for Advanced Study, University of Amsterdam

17 Oude Turfmarkt 147, 1012 GC Amsterdam, the Netherlands

18 ORCID: 0000-0002-9236-6717

19 v.melnikov@uva.nl

20

21 Kay W. Axhausen

22 Institute for Transport Planning and Systems, ETH Zürich

23 CH-8093 Zurich

24 ORCID: 0000-0003-3331-1318

25 axhausen@ivt.baug.ethz.ch

26

27

28 Word Count: 6810 words + 3 table(s) × 250 = 7560 words

29

30 Submission Date: August 2, 2021

**1 ABSTRACT**

2 The importance of walking, the most basic form of transportation, is growing. Climate change,  
3 comfortable walking distances could get reduced drastically. There is a clear need to better under-  
4 stand how outdoor thermal comfort (OTC) and walking interact. In this work, thermoregulation  
5 of the human body is modeled with the two-node model to determine the influence of the micro-  
6 climate on pedestrian's OTC. First, the impact of the current microclimate in Zurich on the route  
7 choice of pedestrians is analyzed. We found no significant correlation between simulated OTC  
8 of walking a particular route and route choices for all trips, but results for longer trips indicate a  
9 possible influence. It is pointed out that the same assessment could be done for other regions, and  
10 results could contribute to more accurate pedestrian modeling. Second, a tool is developed that can  
11 estimate OTC-corrected walking distances from any location. The tool is applied to the current cli-  
12 mate and future climate scenarios. The results show that in the future, pedestrian's OTC in Zurich  
13 will be severely decreased. Further, the tool can detect where there is potential for and, through  
14 its accessibility approach, quantify improvements to the built environment citywide. Future work  
15 should focus on enhancing physiological input parameters to the model. This work provides a  
16 novel use of the two-node model for walking subjects in a citywide assessment.

17

18 *Keywords:* Outdoor Thermal Comfort, Heat Stress, Walkability, Route Choice, Dynamic Thermal  
19 Environment, Climate Change

## 1 INTRODUCTION

2 With the revival and reurbanization of the inner cities around the globe, walking, the most basic  
3 form of transportation, has become a topic of growing interest over the last decade. For certain  
4 use cases, walking can be considered superior to other modes, as it does not come with negative  
5 externalities regarding emissions, landscape aesthetics, and space consumption (1). It further in-  
6 cludes positive externalities on the individual level such as physical and mental health (2) and can  
7 provide recreational value. For urban and transport planners, it is essential to know how to as-  
8 sess whether our cities are walkable and where improvements should be targeted. Following Sim  
9 (3), walkability can be defined as being "about accommodating walking, making it easy, efficient,  
10 and enjoyable." The walkability topic has been extensively addressed by literature (4, 5, 6, 7, 8, 9).  
11 Walkability is for instance enhanced by land-use diversity and density, nearby green areas, and less  
12 traffic. Reflecting on the existing research, one aspect which is often neglected when measuring  
13 walkability is the OTC of the pedestrian. While walkability comprises the influence on the quality,  
14 the term of accessibility stands for the quantitative number of opportunities (10). Low OTC can  
15 restrict walkability and accessibility. Evaluating OTC becomes of growing importance in the face  
16 of the global climate crisis. The official Swiss Climate Change Scenarios (11), indicate potential  
17 temperature increases in the summer months of 6°C for 2060 under the RCP8.5 scenario. Many  
18 studies have modeled OTC for a steady state of walking activities and environmental conditions  
19 (e.g. (12)). The results are typically maps that indicate which places are comfortable and which not  
20 (13). However, none of the existing research has connected OTC, measured with dynamic envi-  
21 ronmental states that are mapped to the spatio-temporal dimension of a given pedestrian trajectory,  
22 to the concept of walkability or accessibility.

23 This paper focuses on the dynamics of OTC for pedestrians in the City of Zurich, Switzer-  
24 land. In a first step, we set up a data processing pipeline allowing us to estimate the OTC employing  
25 the thermoregulatory model from Melnikov et al. (14). We then conduct a descriptive analysis us-  
26 ing real-world GPS pedestrian tracks to investigate how OTC affects the route choice in an urban  
27 environment. Finally, we present an OTC-corrected accessibility planning tool that uses an OTC-  
28 corrected routing engine to predict how far pedestrians can walk comfortably facing current and  
29 predicted temperature conditions. The remaining paper is structured as follows: Section 2 pro-  
30 vides the theoretical foundation of the human thermoregulatory system (HTS), OTC assessment,  
31 and findings on pedestrian route choice. We then present the methodology in Section 3. Section 4  
32 presents the results for the descriptive route choice, Section 5 for the OTC-corrected accessibility  
33 planning. Section 6 discusses and concludes the results.

## 34 RELATED WORK

### 35 Human Thermoregulation & the Two-Node Model

36 In this work, we model the HTS with Melnikov et al. (14) implementation of Gagge's two-node  
37 model (TNM) (15). In the TNM, the human body is divided into two concentric shells, the interior  
38 core with uniform  $T_{cr}$  and the outer skin shell with uniform  $T_{sk}$ . Heat transfer is realized between  
39 these two layers and between the outer shell and the environment. The human body aims to main-  
40 tain  $T_{cr}$  and  $T_{sk}$  steady and can initiate different thermoregulatory control functions to do so. If and  
41 how much  $T_{cr}$  and  $T_{sk}$  deviate from target values is determined by the human heat balance. The  
42 body tries to reach a stable state where the heat storage rate ( $St$ ) is  $St = H_p - H_l \approx 0$ . Both the  
43 produced ( $H_p$ ) and lost heat ( $H_l$ ) are influenced by the individual's characteristics, such as weight  
44 and height, clothing, and especially by the surrounding microclimate. Heat is produced as a result

1 of metabolic activity ( $M$ ), which is not used for mechanical work  $WR$ , and through shivering ( $S_h$ )  
 2 in cold temperatures. The heat production is then  $H_p = M - WR + S_h$  (16). Heat lost by convection  
 3  $C$  (from the skin to the air) and radiative heat exchange  $R$  with surfaces in the environment, through  
 4 respiration  $Re$  (warming and moisturizing inhaled air), and through evaporation of sweat  $E$ . The  
 5 heat loss rate is hence  $H_l = C + R + E + R_e$  (16).

## 6 Skin Wettedness

7 The existing literature reveals that in cold environments, thermal discomfort has a high correlation  
 8 with skin surface temperature. In hot environments or while exercising, it is more related to sweat-  
 9 ing (17, 18). The sweat produced to keep the HTS in balance evaporates. The share of skin surface  
 10 needed to evaporate the produced sweat is called skin wettedness ( $wt$ ) (18). It is a dimensionless  
 11 variable with a minimum value equal to 0.06 because of the moisture diffusion happening through  
 12 the skin and a maximum of 1 when sweat covers the entire skin surface (18). Nishi and Gagge (18)  
 13 found that metabolism due to exercise determines the thermal comfort (TC) limit, resulting in a  $wt$   
 14 threshold ( $wt_{thr}$ ) defined as:

$$wt_{thr} = 0.0012M + 0.15 \quad (1)$$

15  
 16 with  $M$  in  $W/m^2$ . Fukazawa and Havenith (17) confirmed this relation with a study for garment  
 17 design on differences in comfort perception while walking at 4.5 km/h. Also, the results of Lee  
 18 et al. (19) with eight male Japanese subjects walking between 6-8 km/h and the work of Vargas  
 19 et al. (20) with 16 young adults from the US found that the discomfort level follows the relation  
 20 proposed by Nishi and Gagge. In general, when studies assess walking subjects, the  $M$ -dependent  
 21 threshold from Nishi and Gagge (18) is used or referred to.

## 22 Pedestrian OTC Assessment

23 OTC can be defined as "the condition of mind that expresses satisfaction with the outdoor thermal  
 24 environment" (21). There are several metrics to assess OTC, which are based on the TNM. The  
 25 most widely used is the physiologically equivalent temperature (PET) (22). An important feature of  
 26 this index is that it provides a "feels-like" temperature allowing to compare the effect of the micro-  
 27 climate on the thermophysiological state of a person. Further, it considers a steady physiological  
 28 state, which is reasonable for indoor conditions but barely the case for outdoor environments due  
 29 to the significant variance of microclimate conditions and the diverse activities people perform.  
 30 This is why thermal history, dynamic exposure, and the activity of a person are critically important  
 31 to assess instantaneous and dynamic thermophysiological states. Existing studies using the PET  
 32 differ significantly regarding their results on comfortable temperature ranges because they lack the  
 33 just mentioned aspects (23). Some scientists extended the TNM to overcome these fundamental  
 34 limitations. Lai et al. (23) "developed a human heat transfer model that considers outdoor radiative  
 35 heat exchange and transient heat transfer in clothing." Their overall results were satisfying, but dur-  
 36 ing hot conditions, skin temperature prediction error was up to 6°C. An extension of Gagge's TNM  
 37 that is validated for the wide range of warm thermal environments is provided by Melnikov et al.  
 38 (14). With their modified model for skin blood flow, they accurately predicted skin temperature in  
 39 unsteady conditions for measured data on 15 subjects.

## 1 Pedestrian Route Choice

2 Pedestrian route choice has been studied by scholars from different sectors like public health, real  
3 estate, pedestrian interaction modeling, designing of pedestrian infrastructure. From a perspective  
4 of urban- and transport planning, this paper aims to understand how the micro-built environment  
5 affects walking route choice to improve this built environment. Existing studies are either based  
6 on stated (SP) and revealed preference (RP), whereas the latter is considered to provide a better  
7 representation of real-world behavior (6). Numerous studies show that trip length is the primary  
8 determinant to chose a particular route (6). Broach and Dill (5) used 1,167 GPS tracks realized by  
9 283 adults (avg. trip length was 875 m) and compared several route attributes with those of pos-  
10 sible alternatives. They found that higher traffic (+14%), missing crossing infrastructure (+73%  
11 for major roads), and primarily steep uphill gradients (+99%) increase perceived walking time.  
12 Neighborhood commercial reduced the perceived walking time by (-28%). Guo (4) observed sub-  
13 way egress trips and found that steepness and parks have a high effect on utility, while sidewalk  
14 width, intersection density, and neighborhood businesses only have a minor influence. Erath et al.  
15 (8) estimated elasticities for walking time-based on SP and RP data. Amongst other variables, they  
16 found that active window frontage (-17.5%) and relevant greenery reduce perceived walking time  
17 (-23%). A recent study from Salazar Miranda et al. (9) using GPS tracks found that pedestrians  
18 systematically deviate from their shortest path. They do so to walk on streets close to parks, have  
19 more business establishments, and have urban furniture.

20 If humans cannot cope with the stress caused by the microclimate and the physiological  
21 responses, they must adapt their behavior (24). Several studies confirm that pedestrians incorpo-  
22 rate behavioral adjustments to maintain their HTS in balance. Lee (25) found that not  $T_{air}$  but  
23 global radiation (GR) from the sunlight, which determines mean radiant temperature ( $T_{mrt}$ ), was  
24 the reason for people changing the side of the street in a study on four locations in New York City.  
25 A recent study from Singapore (24) examined the effect of shade on path choice. They found that  
26 pedestrians' assumed walking time in the sun was 16% higher than on a shaded path.

## 27 METHODOLOGY

### 28 Estimation of the Microclimate Conditions

29 According to various studies,  $T_{mrt}$  (average temperature of the surfaces that surround a person, with  
30 which the person exchanges thermal radiation) is the driving parameter of human OTC (26) as  $T_{mrt}$   
31 determines the level of radiative heat exchange and varies significantly. Other variables (e.g.,  $T_{air}$ ,  
32  $RH$ ) are steadier in urban environments; thus, there is less chance of them affecting the dynamics  
33 of HTS (16).  $T_{mrt}$  is calculated with the Solar Long Wave Environmental Irradiance Geometry  
34 model (SOLWEIG) (27). The SOLWEIG model is part of the Urban Multi-scale Environmental  
35 Predictor (UMEP), a tool that combines models essential for climate simulations (27). Due to its  
36 3D approach and high level of detail, it can contemplate complex urban situations. Several studies  
37 confirmed the ability of the SOLWEIG tool to predict  $T_{mrt}$  in different places and often better than  
38 its competitor Softwares RayMan Pro or ENVI-met (27, 26). SOLWEIG requires inputs such as  
39 digital elevation models, land cover information, sky view factor (fraction of sky which can be  
40 seen from a given place), meteorological data, and albedo-, emissivity- and absorption-factors of  
41 different materials, all of which are accessible through open data or can be calculated with UMEP's  
42 preprocessors. From all these, the meteorological data represent the essential input for SOLWEIG,  
43 and their derivation required extensive data processing and computation. For the air temperature  
44  $T_{air}$  and relative humidity  $RH$ , the study area is segmented into a 100x100m grid resulting in 5,714

1 patches, i.e. microclimate zones.  $T_{air}$  and  $RH$  are averaged from the three closest out of 28 weather  
 2 stations, weighted by their inverse Euclidean distance.  $T_{air}$  is corrected for altitude differences with  
 3 a vertical temperature gradient of  $0.62^{\circ}\text{C}$  per 100 m (28) due to the hilly topology of Zurich. The  
 4 global radiation  $GR$  is only measured through one sensor for Zurich and hence set constant for all  
 5 microclimate zones. For the final  $T_{mrt}$  calculation, all input data apart from the microclimate zones  
 6 are aggregated to  $2.5 \times 2.5\text{m}$  to keep computation manageable. An example of the result is shown  
 7 in Section 4.1.

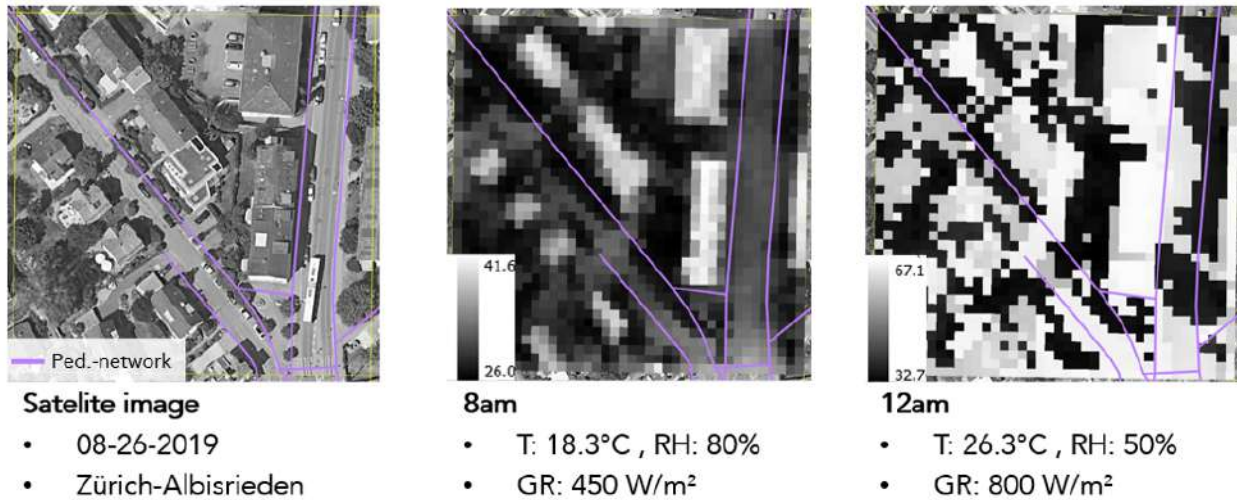


**FIGURE 1:** Mean Radiant Temperature on a  $2.5 \times 2.5\text{m}$  resolution for an example location for 8am and 12am, basemap: (29)

## 8 Model for metabolic and mechanical work rate

9 Metabolic and mechanical work rates are essential variables in the human heat balance.  $M$  and  $WR$   
 10 influence the level of heat gains. While there are simulations considering level walking (23, 14, 30),  
 11 the gradient of the walking surface, which dramatically affects  $M$  and  $W$ , was not previously  
 12 integrated in simulations of pedestrian heat stress. We use equation 1 adapted from Ardigò et al.  
 13 (31) to estimate the metabolic rate  $M$  of walking:

$$15 \quad C_w = 1.866av^2 - 3.773bv + c + 4.456 \quad [\text{J} \cdot \text{kg}^{-1} \cdot \text{m}^{-1}] \quad (2)$$

16  
 17 where  $a = e^{4.911i}$ ,  $b = e^{3.416i}$ ,  $c = 45.72i^2 + 18.9i$ , with  $i$  being the gradient in % and  $v$  is speed in  
 18 m/s and add the resting metabolic cost from Since Ardigò *et al.*'s formula only accounts for the  
 19 walking part of metabolic cost ( $M_{base}$ ), of  $1.00108 [\text{W} \cdot \text{kg}^{-1}]$  (32) to  $C_w$ .

20 The mechanical work  $WR$  for walking can be divided into two parts: 1. external work  
 21 ( $WR_{ext}$ ) "necessary to sustain the displacement of the center of mass of the body (COM) relative  
 22 to the surroundings", 2. internal work ( $WR_{int}$ ) "done to move the limbs relative to the COM"  
 23 and "work done by the trailing limb against the leading limb during double support" (33). We  
 24 developed a new model to estimate speed and gradient dependent  $WR$  based on two studies. Values  
 25 for  $WR_{int}$  are taken from Minetti et al. (34) and  $WR_{ext}$  is provided by the study of Dewolf et al. (33).

- 1 Their data points are fitted separately with polynomial regressions, and then they are summed up.
- 2 Both mechanical work rate and metabolic rate for walking speeds considered in this re-
- 3 search are shown in Section 4.2.

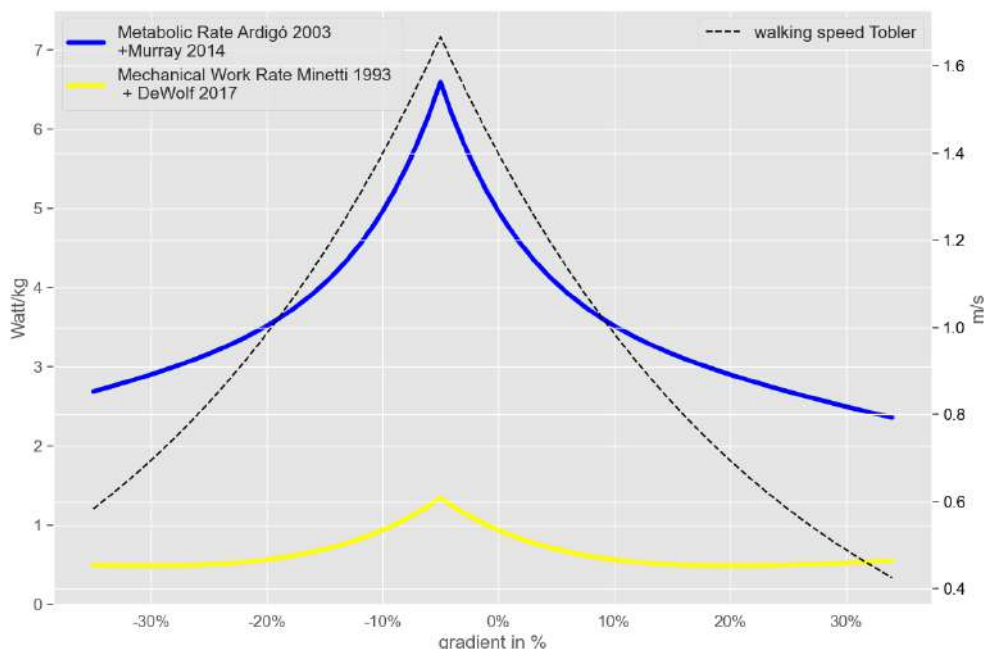


**FIGURE 2:** Estimated model of metabolic rate and mechanical work rate for different gradient-walking speed pairs

#### 4 Pedestrian Route Choice

##### 5 *Network and Enrichment*

6 OSMnx is used to create a routable network from the pedestrian network provided by the City  
 7 of Zurich. The pedestrian network used is composed of 54,608 edges and 17,582 nodes. With  
 8 the elevation data sourced from the Google API (29) the gradient of each edge is calculated. The  
 9 network is enriched with several attributes which have been identified as relevant from the literature  
 10 (see: Section 4.3.1). The built environment attributes are sourced from OpenStreetMap (OSM)  
 11 and the City of Zurich. The attributes include 4,639 business establishments (containing shops  
 12 and food and beverage facilities), 7,867 urban furniture elements (including benches, trash bins,  
 13 drinking water fountains, and public toilets), 73,042 trees (registered in the public cadaster), and  
 14 neighboring parks and urban forests. All attributes are assigned to the corresponding edges of  
 15 the pedestrian network if they are in a range of 10m. Furthermore, the network is enriched with  
 16 the average weekday traffic (AAWT, in the following traffic), provided by (35) with around 60%  
 17 network coverage. The traffic data contains the streets' centerline and is assigned to the edges using  
 18 a 20m range. Finally, the share of conveniently walkable gradients that is conveniently walkable  
 19 gradient is defined as -5% to 1% because of the ratio between  $M$  and  $WR$  rate, is encoded based on  
 20 the network topology.

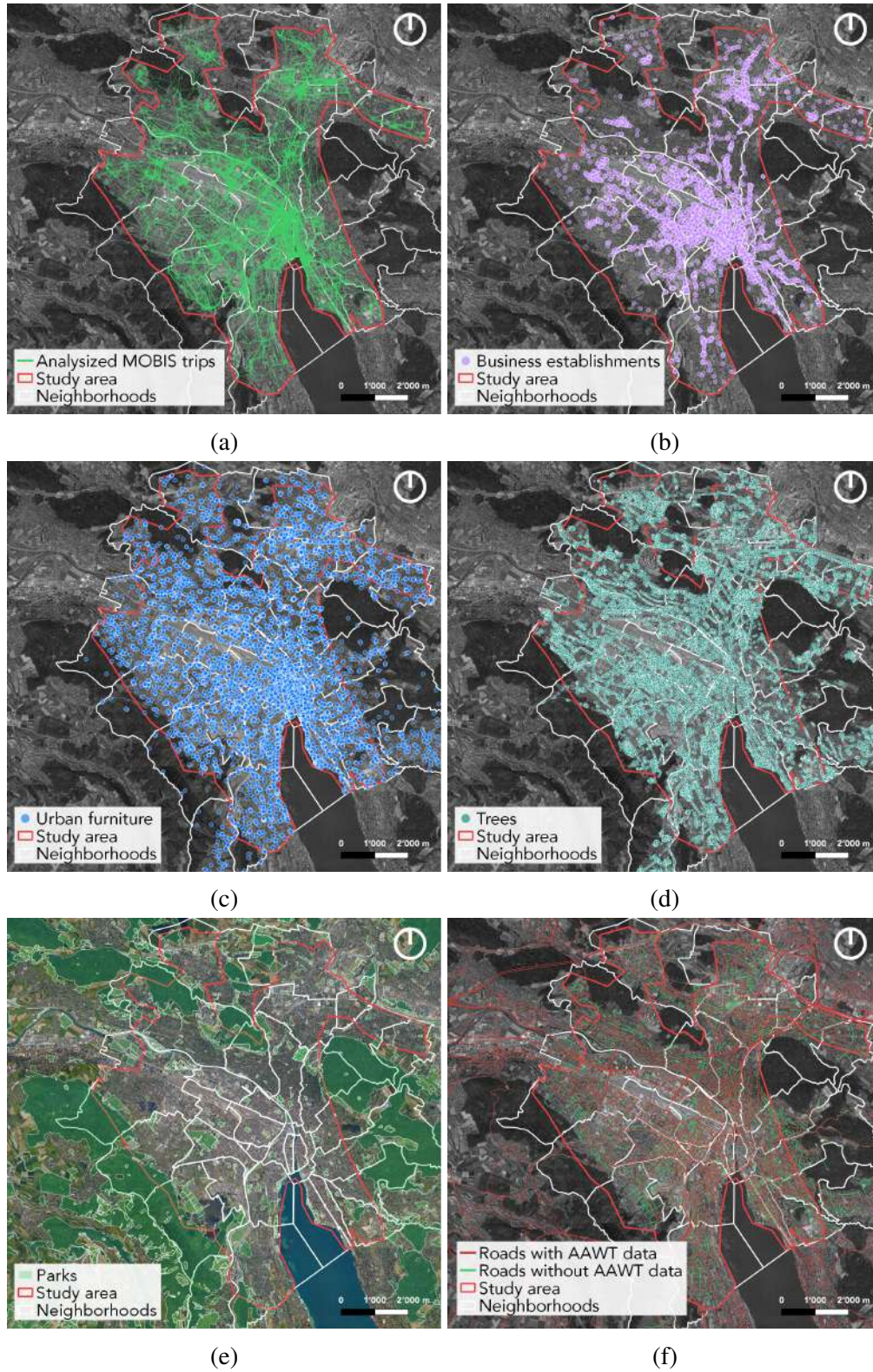


**FIGURE 3:** Study area (a), built environment attributes: business establishments (b), urban furniture (c), trees (d), parks and urban forests (e), and AAWT (f)



### 1 *Pedestrian's Trajectory Data*

2 The trajectory data used for this work comes from the MOBIS-covid project, an app-based GPS-  
 3 tracking travel diary study (36). The built environment and OTC-related attributes of these trajec-  
 4 tories are compared to the same attributes of the shortest path of the respective origin-destination  
 5 pair. The study area does not contain the whole city of Zurich (see Section 4.3.1 (a)) but only the  
 6 parts which contain the majority (94%) of the trajectories due to the computational constraints.  
 7 The 70 warmest days in 2020 are selected for the analysis. For the 70 days, the microclimate is  
 8 calculated between 8:00 AM and 8:00 PM in 90-minute steps due to computational capacity of the  
 9  $T_{mrt}$  calculation, resulting in nine points of time in a day and a total of 630 microclimates for each  
 10 microclimate zone. Trips shorter than 200 m are removed because they are too short to obtain a  
 11 satisfactory result on OTC in Zurich's climate. Moreover, paths where the start and endpoint are  
 12 less than 200 m apart are sorted out because they are likely to be roundtrips. Hence the shortest  
 13 path comparison would yield misleading results. The remaining trips are matched to the pedestrian  
 14 network, using a Hidden Markov Model-based map matching framework from Meert and Verbeke  
 15 (37). Then, the microclimate zones (100x100m) and the  $T_{mrt}$  cells (2.5x2.5m) are assigned to the  
 16 trips based on time and location. In many cases, trajectories lie in more than one microclimate zone  
 17 or  $T_{mrt}$  cell. In this case, the trajectory is cut, and each part of the segment is assigned to its cor-  
 18 responding microclimate zone and  $T_{mrt}$  cell. To not further increase computation times, the wind  
 19 data is mapped on each trajectory segment's centroid. The final sample of trajectories contains  
 20 2'660 trips, realized by 333 different individuals, of which 59% are female, with an average age of  
 21 43 years. To initialize the thermoregulatory model, average weight and height for gender-age pairs  
 22 of the participants are determined from the national health survey 2017 (38). The clothing level  $I_{CL}$   
 23 is estimated through the linear function  $I_{CL} = 1.625 - 0.0375T_{air}$ , obtained from Melnikov et al.  
 24 (30).

### 25 **OTC-Corrected Accessibility Planning**

#### 26 *Implementation of the Tool*

27 The developed tool enables users to calculate the OTC-corrected maximum walking area from  
 28 every given point in the city. Also, here the pedestrian network of the City of Zurich is used, but  
 29 the maximum edge length is set to 30m to get more accurate results. To calculate the isochrones  
 30 from each point of interest, the shortest paths are calculated to all other nodes in the network,  
 31 reachable in a defined walking time. The walking speed is assumed to be gradient-dependent,  
 32 defined by Tobler's hiking function (39). The assignment of the microclimate to the network and  
 33 the clothing are done in the same way as described in Section 4.3. Additionally, it is assumed  
 34 that  $T_{mrt}$  is equal to  $T_{air}$  if the edge is inside a building. The weight of the assessed individual  
 35 is assumed to be 72.3kg and height 1.71m which represents the average Swiss citizen (38). The  
 36 metabolic dependent  $wt$  threshold is calculated with Eq. (1). The trajectory's segments have an  
 37 average length of just 2.8 m.  $M$  depends on speed and gradient, and they are different for every  
 38 segment of the trajectory. The threshold would hence fluctuate a lot, and it would be unrealistic to  
 39 assume that someone stops walking when the threshold  $wt_{thr}$  is reached for a fraction of the whole  
 40 trip. Hence, it is decided to calculate the threshold based on the weighted mean of the edges from  
 41 the  $\approx 80$  s. The paths are then cut when the threshold  $wt_{thr}$  is exceeded. The tool's code will be  
 42 made available to interested colleagues on request.

## 1 Use Cases & Scenarios

2 The tool's usefulness is demonstrated by evaluating two of the municipality's community centers  
 3 for different climate scenarios. One community center (CC) is "Bäckeranlage," a dense urban dis-  
 4 trict with relatively narrow street canyons. The other is "Oerlikon," selected because new develop-  
 5 ments on former industrial production sites representing contemporary common building practice  
 6 are within a 20-minute walking radius. The area enclosing all comfortable reachable edges, and  
 7 the number of persons living in this area within 20 minutes walking time is assessed.

8 The tool draws on estimating the thermoregulatory model and derivation microclimate  
 9 zones from the previous route choice analysis. Scenarios Median and Hottest are based on the  
 10 already computed microclimate for the 70 warmest days in 2020. As mentioned earlier, the num-  
 11 ber of hot days ( $> 30^{\circ}\text{C}$ ) and the average daily maximum temperatures are expected to increase  
 12 drastically in the future. We hence additionally evaluate the climate scenarios under RCP4.5 and  
 13 RCP8.5 for 2060. The mean daily maximum temperature increase in August from these scenarios  
 14 ( $3.5^{\circ}\text{C}$  for RCP4.5 and  $5.6^{\circ}\text{C}$  for RCP8.5) is added to the hottest measured temperature of 2020.  
 15 The represented quantitative and qualitative evaluation focuses on the time of day with the highest  
 16 solar radiation, and thus highest  $T_{mrt}$ , i.e., 12:30. The specific scenarios are as follows:

17

18 **Scenario Median** the median (50% higher, 50% lower),  $T_{air}$  at 12:30PM (09-09-20):  $24.7^{\circ}\text{C}$

19 **Scenario Hottest** the hottest day,  $T_{air}$  at 12:30PM (11-08-20):  $31.4^{\circ}\text{C}$

20 **Scenario 2060 RCP4.5** the hottest day in 2060, considering scenario RCP 4.5 (11),  $T_{air}$  at 12:30  
 21 PM:  $34.9^{\circ}\text{C}$

22 **Scenario 2060 RCP8.5** the hottest day in 2060, considering scenario RCP 8.5 (11),  $T_{air}$  at 12:30  
 23 PM:  $37.0^{\circ}\text{C}$

## 24 RESULTS ON ROUTE CHOICE OF MOBIS-COVID TRIPS

### 25 Thermal Comfort

26 Table 1 shows the comparison between the statistics of the chosen and shortest path. Mean  $T_{air}$  and  
 27  $T_{mrt}$  are almost identical. The average mean and maximum level of  $wt$  experienced during trips  
 28 are higher for chosen paths. Also, the share of chosen paths with a higher mean and maximum  
 29  $wt$  was higher, which is not surprising: For the 70 warmest days that this paper is considering, the  
 30 body must compensate for excess heat during almost the entire path (97.5%). Hence,  $wt$  increases  
 31 steadily during a trip because the body's core and skin temperature increases steadily, making  
 32 increased heat losses in the form of evaporation necessary (see Section 5.1). The chosen paths  
 33 are an average of 89 seconds/123 meters longer, meaning that the body continues sweating during  
 34 this surplus time with higher  $T_{cr}$  and  $T_{sk}$ , resulting in the higher mean and maximum  $wt$  value for  
 35 chosen paths. The results in a subset with trips where the chosen path is less than 10% longer than  
 36 the shortest path confirm the hypothesis that higher  $wt$  is due to longer trips. In these cases, the  
 37 mean and median for both  $wt$  variables are almost identical, and no more significant differences  
 38 can be revealed. The ranges of maximum  $wt$  are on a level that does not cause strong thermal  
 39 discomfort, and the  $wt_{thr}$  threshold of 0.38 ( $M=190\text{W}/\text{m}^2$ ,  $v=1.4\text{m}/\text{s}$ ) is exceeded for only three  
 40 trips. The short mean walking time (chosen paths:  $\sim$ nine minutes, shortest paths:  $\sim$ eight minutes)  
 41 together with the temperatures present for the MOBIS-covid data (mean  $T_{air}$  is  $25^{\circ}\text{C}$ ), leads to  
 42 the conclusion that anticipation of level of thermal comfort is not considered by the participants  
 43 in the process of route choice. This might be both due to relatively comfortable overall thermal  
 44 conditions and smaller possible differences in thermal experience in such a short period. However,

**TABLE 1:** Overall results chosen path vs. shortest path: Compared are the mean, median, and standard deviation of the attributes for all trips. The share of chosen paths with a higher, the same, or lower value for the attribute than its corresponding shortest path is stated. The distribution of the attributes' means is- compared between chosen and shortest paths with two statistical tests.

attribute	chosen path			shortest path			% of chosen value is ... than shortest		
	mean	median	std.	mean	median	std.	>	=	<
mean skin wet. <sup>*/#</sup>	0.137	0.13	0.03	0.129	0.123	0.029	87.3	0	12.7
max skin wet. <sup>*/#</sup>	0.182	0.173	0.046	0.171	0.162	0.044	85.4	0.2	14.4
mean $T_{air}$ in °C	25.14	25.30	3.50	25.14	25.3	3.496	48.5	3.5	47.9
mean $T_{mrt}$ in °C	37.72	38.38	11.43	37.76	38.04	11.60	50.4	0	49.5
length in m <sup>*/#</sup>	756	603	504	633	503	431	98.5	0	1.4
time in s <sup>*/#</sup>	549	439	368	460	365	315	99.9	0	0
traffic	3,139	2,478	2,735	3,272	2,523	2,907	43.9	3.3	52.8
% of flat	74.6	81.7	24.8	74	81.4	26.2	50	10	39.9
no. busin./100 m	2.539	1.614	2.777	2.61	1.608	2.927	40	11.9	48.1
no. urb. furn./100 m <sup>*</sup>	1.036	0.791	0.926	0.992	0.727	0.944	43	6.7	50.3
% along park	12.4	0	20.4	11.9	0	20.4	21.6	52.8	25.6
no. trees/100 m <sup>*/#</sup>	2.878	2.316	2.707	2.78	2.132	2.752	43.9	10.2	45.9

n=2,061, chosen = shortest path: 598, 64.3% of the chosen route is different from shortest route,  
<sup>\*/#</sup>=significant on  $\alpha=0.05$  for Mann-Whitney-U-/Two-sample Kolmogorov–Smirnov-Test

**TABLE 2:** Results for longer trips: The mean value of each attribute is compared between chosen and shortest path for subsets of trips with different minimum lengths. Statistical tests are applied to compare the distribution of the mean for each attribute.

	>696 m (n=609)			>1,100 m (n=203)			>1,500 m (n=96)		
	mean ch.	sh.	MWU/ KS2S	mean ch.	sh.	MWU/ KS2S	mean ch.	sh.	MWU/ KS2S
mean skin wet.	0.166	0.159	*/#	0.193	0.185	*	0.209	0.202	
max skin wet.	0.226	0.216	*/#	0.261	0.252		0.282	0.276	
mean $T_{air}$ in °C	25.20	25.19		25.23	25.24		24.79	24.80	
mean $T_{mrt}$ in °C	36.87	37.04		38.15	38.50		39.39	40.07	
length in m	1,300	1,126	*/#	1,898	1,653	*/#	2,365	2,084	*/#
time in s	945	819	*/#	1,378	1,203	*/#	1,713	1,512	*/#
traffic	3,534	3,848	*	3,663	3,939		3,621	4,037	*/#
% of flat	72.8	71.7		69.3	68.1		68.6	68.3	
no. busin./100 m	1.987	2.013		1.478	1.666		1.387	1.506	
no. urb. furn./100 m	1.047	0.946	*	0.965	0.864		0.867	0.775	
% along park	17.1	15.8		18.3	16.6		17.0	15.8	
no. trees/100 m	3.382	3.054	*	3.528	3.034	*	3.787	3.269	*

ch. = chosen path, sh. = shortest path, \*/#=significant on  $\alpha=0.05$  for Mann-Whitney-U-(MWU) / Two-sample Kolmogorov–Smirnov-Test (KS2S)

1 the results in Table 2 indicate that for longer trips, thermal comfort might play an increasing role  
 2 in the participant’s route choice. Mean and maximum  $wt$  of chosen paths compared to shortest  
 3 paths are becoming more similar the longer trips are. For trips longer than 1,500 m, the values of  
 4 mean and maximum  $wt$  for both paths sets are almost equal, despite the more than three minutes  
 5 longer walking time for chosen paths, where  $wt$  continues to increase steadily. Another indicator  
 6 for a conscious OTC-seeking route choice behavior in the lower  $T_{mrt}$  for chosen paths compared  
 7 to shortest paths, which gets higher with increasing trip lengths (by 0.17°C for trips>696 m, by  
 8 0.35°C for trips>1,100 m and by 0.68°C for trips>1,500 m).

## 9 Built Environment and General Observations

10 In general, participants of the MOBIS-covid study prefer longer paths for their trips, both in terms  
 11 of length and travel time. Also, for only 22.5% of the trips, people chose the shortest path. For the  
 12 trips where the chosen path is different from the shortest path, 64.3% of the chosen route’s length  
 13 is different from the shortest route meaning chosen paths are substantially different. In the overall  
 14 results (see Table 1), all attributes of the built environment except business establishments have  
 15 higher (respectively traffic lower) mean values for chosen paths when compared to the shortest  
 16 ones. For the number of urban furniture (WMN) and trees, the distribution of the mean is signifi-  
 17 cantly different (WMN&KS2S). Nevertheless, only for traffic and percentage of flat gradients, the  
 18 chosen paths have a higher share of lower (for traffic) respectively higher values (for the percentage  
 19 of flat gradients).

20 It was found that for longer trips, the built environment gains importance. In Table 2 it can

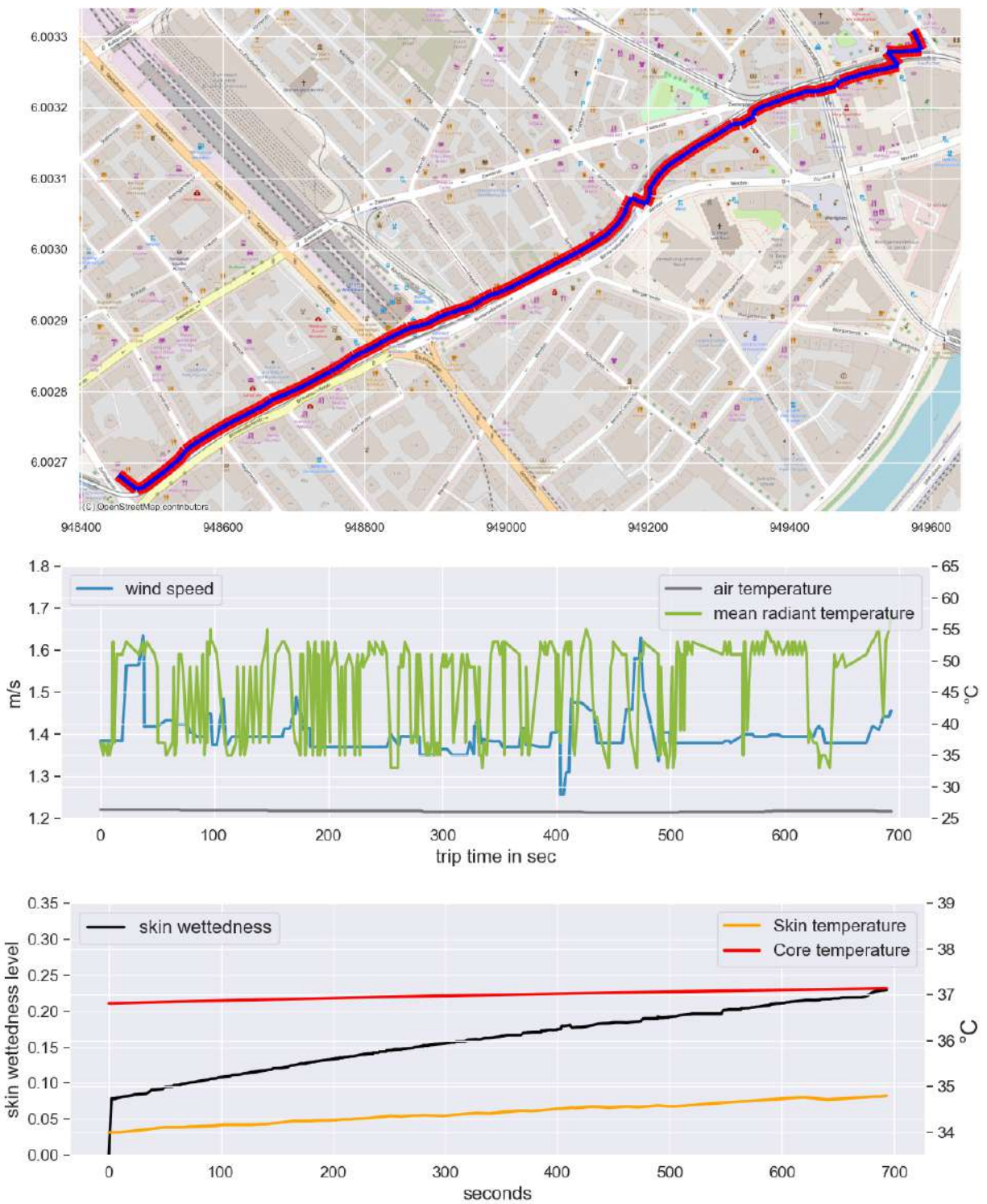


**FIGURE 4:** Exemplary path, top: Trajectory, center: Air- and mean radiant temperature, and wind speed; bottom: Skin wettedness, core- and skin temperature

1 be seen that the difference between the values of the attributes for chosen and shortest path get  
2 more pronounced for longer trips. For example, the traffic for chosen paths considering the overall  
3 results is approximately 100 vehicles/h less than for the shortest paths. At the same time, there are  
4 around 300 fewer vehicles/h for the subset of trips where the shortest path is longer than 696m. The  
5 same pattern can be observed for the other attributes, except for business establishments which are  
6 consistently higher for shortest paths, contrary to findings of previous studies. The share of chosen  
7 paths with higher (for traffic lower) mean values is higher for traffic, the percentage flat gradients,  
8 the number of trees, and urban furniture, when considering longer trips. For the percentage of trips  
9 along a park, the share of chosen paths with higher values is slightly lower. The mean number of  
10 trees, percentage of trip along parks, percentage of flat gradients, and traffic are higher than the  
11 overall results for longer trips. This can be explained by that the probability of passing by green  
12 areas and busier roads for longer trips is higher, and the likelihood for steeper gradients is higher  
13 for longer trips. The number of urban furniture and business establishments is lower because there  
14 are fewer businesses and urban furniture along green areas.

15 The analysis of the MOBIS-covid data showed that currently, OTC has a limited influence  
16 on route choice in Zurich. This is partly because an insufficient number of trips were done under  
17 temperatures that noticeably negatively affect OTC, and the length of the trips was short. This is  
18 confirmed by the results presented in Section 6, where it was found that the current climate has a  
19 weak influence on the OTC-corrected walking distance for trips up to 20 minutes. Nevertheless,  
20 longer trips showed that OTC could potentially play a role in the route choice, but the low samples-  
21 size (96) impedes secure conclusions. The designed methodology to assess OTC for the travel diary  
22 trips is novel, supporting that such estimation can be done with existing models and data, even on  
23 a citywide level. Regarding the built environment attributes, it was shown that these become more  
24 important for longer trips.

## 25 **RESULTS ON OTC-CORRECTED ACCESSIBILITY**

26 Table 3 shows the statistics for the different scenarios for the two community centers. For the  
27 median scenario, the area and population for both CCs are not affected at all (see Section 6).  
28 CC Bäckeranlage is almost unaffected by the hottest scenario. In contrast, CC Oerlikon shows  
29 some (minor) reductions for the area and population inside this area. Also, for the more moderate  
30 RCP4.5 scenario, reductions for Oerlikon are more pronounced: ca. 15% of the area is reduced,  
31 and population inside the area decreases by 13.4%. The losses are all located at the fringes of  
32 the walkable radius, which is intuitive because  $w_t$  steadily increases in hot conditions. The de-  
33 crease in the area (-10.6%) and population inside this area (-5.2%) for CC Bäckeranlage for the  
34 same scenario is smaller. In the RCP8.5 scenario for CC Oerlikon, the decrease of area (-42.7%)  
35 and population inside the area (-36.1%) is more pronounced. For the new urban developments,  
36 no striking differences compared to the rest of the urban fabric can be observed. Compared to  
37 CC Bäckeranlage, the comfortable walking paths are reduced spatially more uniformly. For CC  
38 Bäckeranlage, the area is reduced by over 50%, and the population inside the area decreases by  
39 almost 40%. This can be explained by the high building density and extensive impervious sur-  
40 faces present, which is further confirmed with higher  $T_{air}$  (CC Bäckeranlage: 37.2°C, CC Oerlikon  
41 36.5°C). The difference between scenario RCP4.5 and RCP8.5 for both CCs is notable because,  
42 in the RCP8.5 scenario, heat loss through convection is minimized due to warmer  $T_{air}$  than  $T_{sk}$  for  
43 many time steps. For some time steps, heat convects from the air to the human body. See Section 6  
44 for an example trajectory. Increased sweat production tries to compensate for this, resulting in a

**TABLE 3:** Statistics on CC Bäckeranlage and CC Oerlikon

		area in km <sup>2</sup>			population inside area		
		before	after	$\Delta$	before	after	$\Delta$
<b>CC Bäckeranlage</b>	<b>median</b>	5.08	5.08	0 ( $\pm 0\%$ )	59,421	59,421	0 ( $\pm 0\%$ )
	<b>hottest</b>	5.08	5.06	-0.02 (-0.3%)	59,421	59,421	0 ( $\pm 0\%$ )
	<b>2060: RCP4.5</b>	5.08	4.54	-0.54 (-10.6%)	59,421	56,342	-3,079 (-5.2%)
	<b>2060: RCP8.5</b>	5.08	2.26	-2.82 (-55.5%)	59,421	36,651	-22,770 (-38.3%)
	<b>median</b>	4.89	4.89	0 ( $\pm 0\%$ )	41,711	41,711	0 ( $\pm 0\%$ )
<b>CC Oerlikon</b>	<b>hottest</b>	4.89	4.71	-0.18 (-3.5%)	41,711	40,138	-1,573 (-3.8%)
	<b>2060: RCP4.5</b>	4.89	4.14	-0.75 (-15.3%)	41,711	36,141	-5,570 (-13.4%)
	<b>2060: RCP8.5</b>	4.89	2.8	-2.09 (-42.7%)	41,711	26,644	-15,067 (-36.1%)
	<b>median</b>	4.89	4.89	0 ( $\pm 0\%$ )	41,711	41,711	0 ( $\pm 0\%$ )
	<b>hottest</b>	4.89	4.71	-0.18 (-3.5%)	41,711	40,138	-1,573 (-3.8%)

1 faster exceeding of  $w_{thr}$  limit. For both scenarios, radiation is negative (meaning that heat is not  
2 lost but gained by the body) because  $T_{mrt}$  is always higher than the body's skin temperature. Very  
3 high  $T_{mrt}$  values due to missing shading on big intersections before and on bridges lead to many  
4 paths ending at these places in the RCP8.5 scenario.

5 We demonstrated that OTC is not harmed under current climate conditions but will be  
6 reduced so severely in the context of future climate change that comfortable walking areas are  
7 diminished. The incorporation of shading in bridge design could significantly increase the range  
8 of thermally comfortable walks. The low  $RH$  in Zurich (ca. 40% for the hottest scenario), despite  
9 the high temperatures in the hottest scenario, helps efficient dissipation of heat through evaporation,  
10 explaining the small negative impact of the current climate on OTC. We simulated a hypothetical  
11 scenario of 75% relative humidity (typical for tropical cities like Singapore). The results reveal the  
12 significant impact of  $RH$  on comfortable walking (see Section 6). The reachable area is reduced by  
13 80% and the population inside this area by 70%. This represents more significant decreases than  
14 the 2060 RCP8.5 scenario and can be explained by the reduced possibility of losing heat through  
15 evaporation.

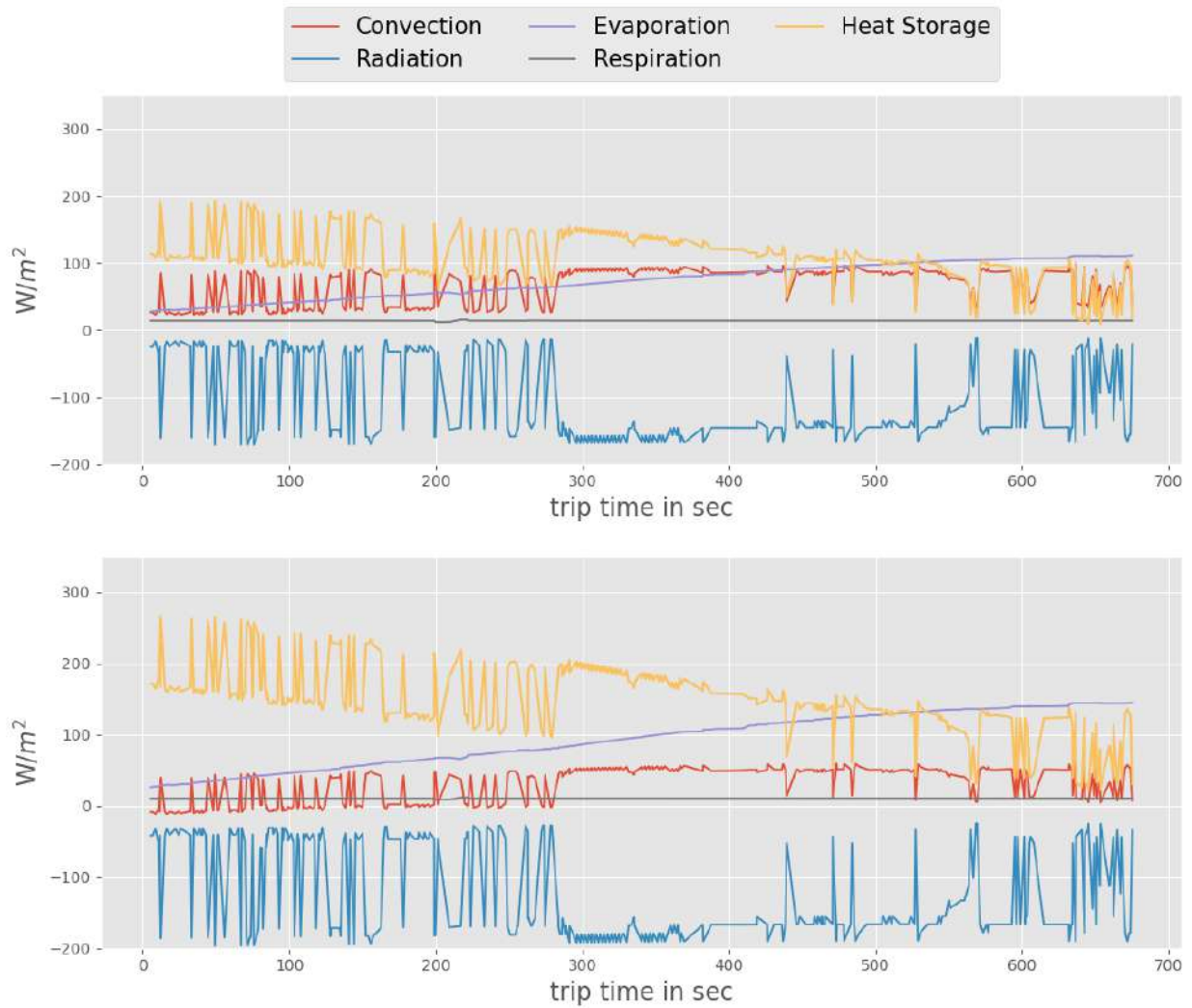


**FIGURE 5:** Human heat balance for an exemplary path (without  $M$  and  $WR$ ), top: scenario hottest, bottom: scenario 2060 RCP8.5, positive values= heat losses, negative values= heat gains



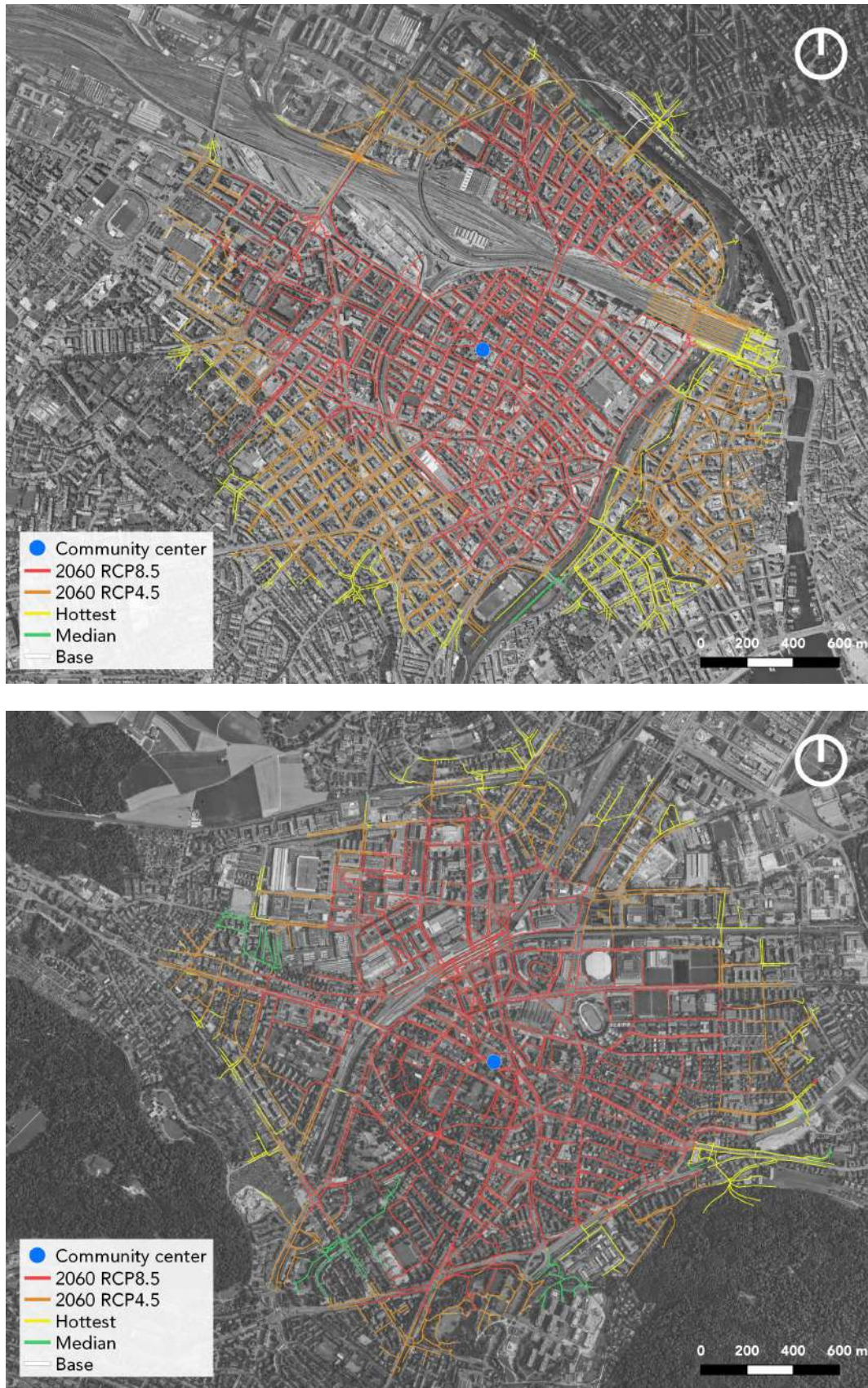


**FIGURE 6:** Comfortable reachable streets for different scenarios, top: CC Bäckeranlage, bottom: CC Oerlikon, basemap: (29)

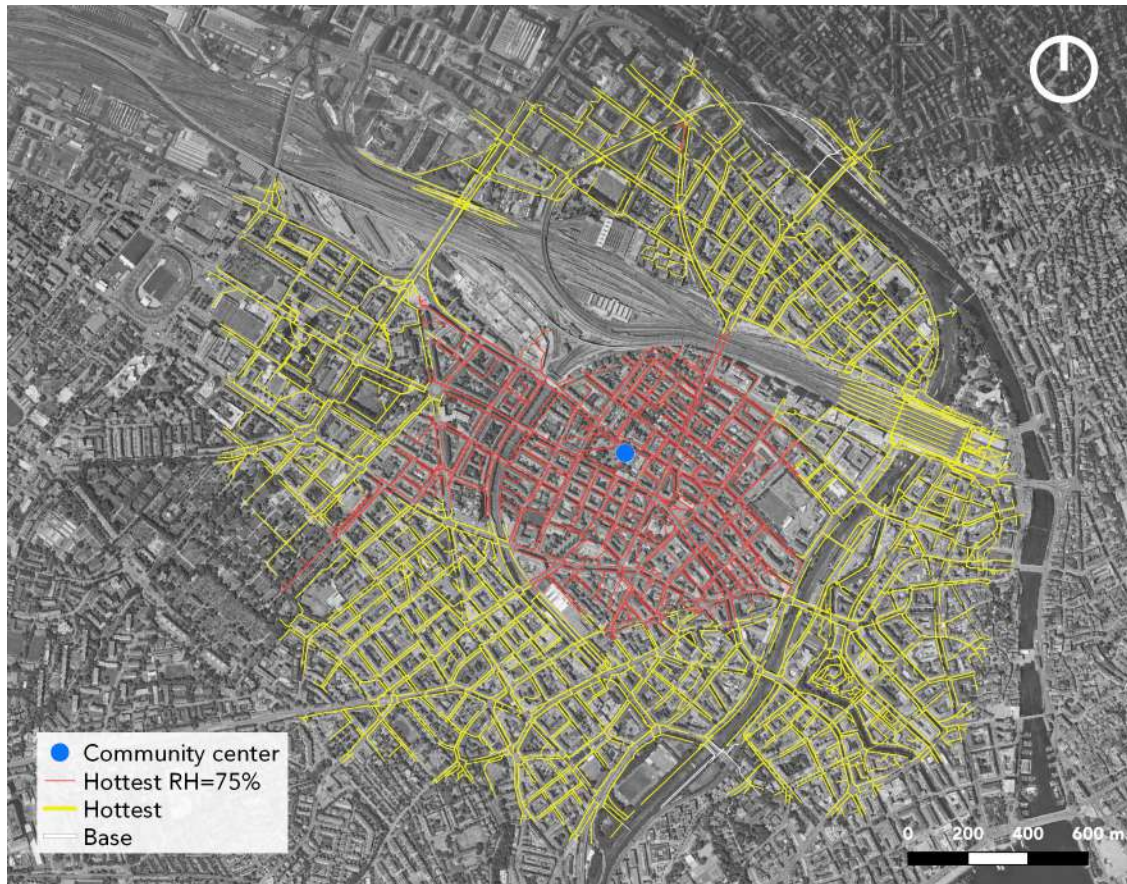


**FIGURE 7:** Comfortable reachable streets, sensitivity on relative humidity: CC Bäckeranlage, basemap: (29)

## 1 CONCLUSION

2 The research at hand applied a human thermoregulation model to comprehensive real-world data.  
3 On the one hand, we assessed OTC for the trips of a travel diary study and found that the pedestrian  
4 path choices in the current climate of Zurich do not suggest that pedestrians integrate anticipated  
5 heat stress in their path planning. There are indications that they do for longer trips, but the sample  
6 size is too small to draw robust conclusions. Nevertheless, the developed methodology can be used  
7 for other study cases where climate might significantly influence route choice. Most important,  
8 it was shown that this is possible with existing, mainly publicly available data. Extending this  
9 work by modeling the route choice using discrete choice models would provide additional valuable  
10 findings. These insights could be implemented in software to model pedestrians more accurately  
11 in hot temperatures. Furthermore, the results could be used to incorporate OTC in navigation  
12 software such as Google Maps.

13 Further, we developed a tool to assess OTC-corrected accessibility based on an OTC-  
14 corrected routing engine. We evaluated its usefulness for two case study locations in Zurich.  
15 It could be shown that the current climate does not affect accessibility thanks to relatively low  
16 *RH*. A sensitivity analysis showed that high relative humidity reduces OTC severely during hot  
17 temperatures. The results for the climate forecasted for 2060 showed remarkable reductions in  
18 OTC-corrected accessibility. In general, the developed tool can be employed in the analysis stage  
19 of projects that aim to secure the outdoor thermal comfort of urban dwellers by indicating the need  
20 for improvements spatially. A great advantage compared to the existing methods of OTC assess-  
21 ment (13) is the accessibility approach which permits quantifying the impact of interventions in  
22 terms of gain in comfortable walking areas or inhabitants for a given location. By modifying the  
23 parameters of the thermoregulation model, outdoor thermal comfort could also be assessed for  
24 particular groups of people and the public infrastructure related to them.

25 Despite the demonstrated contributions, some limitations have to be mentioned. The biggest  
26 one is that for the modeling, it is assumed that pedestrians walk precisely on the centerlines of the  
27 coded pedestrian network. In reality, pedestrians almost always have a margin where to walk on  
28 the sidewalk. This can drastically affect the pedestrian's OTC. The same issue also affects the  
29 behavior on public squares, where not all possible crossing possibilities are represented in the net-  
30 work. Furthermore, the threshold  $w_{t_{hr}}$  used in this work depends on  $M$ . It is the mostly used in  
31 research, but its explanation is insufficient.

32 The presented work is not only of interest for practitioners and researchers in regions with  
33 harsher climates but due to the future increase of global temperatures, especially also for places  
34 where there is still time to react and implement adaptation measures to ensure attractiveness of the  
35 most fundamental transport mode: walking.

## 36 AUTHOR CONTRIBUTIONS

37 The authors confirm contribution to the paper as follows: study conception and design: J. Hess;  
38 data collection: J. Hess; analysis and interpretation of results: J. Hess, K.W. Axhausen, V. Mel-  
39 nikov, A. Meister; draft manuscript preparation: J. Hess; manuscript review: K.W. Axhausen,  
40 A, Meister, V. Melnikov. All authors reviewed the results and approved the final version of the  
41 manuscript.

**REFERENCES**

1. H. Knoflacher. *Fussgeher- und Fahrradverkehr: Planungsprinzipien*. Böhlau, Wien, 1995.
2. L. D. Frank and P. O. Engelke. The built environment and human activity patterns: Exploring the impacts of urban form on public health. *Journal of Planning Literature*, 16(2): 202–218, 2001.
3. D. Sim. *Soft City: Building Density for Everyday Life*. Island Press, Washington D.C., 2019.
4. Z. Guo. Does the pedestrian environment affect the utility of walking? A case of path choice in downtown Boston. *Transportation Research Part D: Transport and Environment*, 14(5):343–352, 2009.
5. J. Broach and J. Dill. Where do people prefer to walk? Pedestrian route choice model developed using GPS data. In *Active living research conference*, San Diego, 2015.
6. Z. Guo and B.P.Y. Loo. Pedestrian environment and route choice: Evidence from New York City and Hong Kong. *Journal of Transport Geography*, 28:124–136, 2013.
7. R. Ewing and R. Cervero. Travel and the built environment. *Journal of the American Planning Association*, 76(3):265–294, 2010.
8. A Erath, M. A. B. van Eggermond, S. A. Ordóñez, and K. W. Axhausen. Introducing the pedestrian accessibility tool: Walkability analysis for a geographic information system. *Transportation Research Record: Journal of the Transportation Research Board*, 2661(1): 51–61, 2017.
9. A. Salazar Miranda, Z. Fan, F. Duarte, and C. Ratti. Desirable streets: Using deviations in pedestrian trajectories to measure the value of the built environment. *Computers, Environment and Urban Systems*, 86:101563, 2021.
10. W. G. Hansen. How accessibility shapes land use. *Journal of the American Institute of Planners*, 25(2):73–76, 1959.
11. National Centre for Climate Services. CH2018 – Klimaszenarien für die Schweiz, 2018.
12. A. H. A. Mahmoud. Analysis of the microclimatic and human comfort conditions in an urban park in hot and arid regions. *Building and Environment*, 46(12):2641–2656, 2011.
13. D. Lai, D. Guo, Y. Hou, C. Lin, and Q. Chen. Studies of outdoor thermal comfort in northern China. *Building and Environment*, 77:110–118, 2014.
14. V. Melnikov, V. V. Krzhizhanovskaya, M. H. Lees, and P. M.A. Sloom. System dynamics of human body thermal regulation in outdoor environments. *Building and Environment*, 143:760–769, 2018.
15. A. P. Gagge, J. Stolwijk, and Y. Nishi. An effective temperature scale based on a simple model of human physiological regulatory response. *ASHRAE Transactions*, 77:247–262, 1971.
16. G. Havenith. Interaction of clothing and thermoregulation. *Exogenous Dermatology*, 1(5): 221–230, 2002.
17. T. Fukazawa and G. Havenith. Differences in comfort perception in relation to local and whole body skin wettedness. *European Journal of Applied Physiology*, 106(1):15–24, 2009.
18. Y. Nishi and A. P. Gagge. Effective temperature scale useful for hypo- and hyperbaric environments. *Aviation, space, and environmental medicine*, 48(2):97–107, 1977.
19. J.-Y. Lee, K. Nakao, and Y. Tochihara. Validity of perceived skin wettedness mapping to evaluate heat strain. *European Journal of Applied Physiology*, 111(10):2581–2591, 2011.

20. N. T. Vargas, C. L. Chapman, B. D. Johnson, R. Gathercole, and Z. J. Schlader. Skin wettedness is an important contributor to thermal behavior during exercise and recovery. *American journal of physiology. Regulatory, integrative and comparative physiology*, 315(5):925–933, 2018.
21. ASHRAE. *ANSI/ASHRAE Standard 55 - Thermal Environmental Conditions for Human Occupancy*. 2017.
22. P. Höppe. The physiological equivalent temperature - A universal index for the biometeorological assessment of the thermal environment. *International Journal of Biometeorology*, 43(2):71–75, 1999.
23. D. Lai, X. Zhou, and Q. Chen. Measurements and predictions of the skin temperature of human subjects on outdoor environment. *Energy and Buildings*, 151:476–486, 2017.
24. V. R. Melnikov, V. V. Krzhizhanovskaya, M. H. Lees, P. M. A. Sloom, and G. I. Christopoulos. Sun discounting mechanisms associated with pedestrian path choices in tropical climates: a quasi-experimental and computational modelling approach. Preprint submitted to Nature Human Behaviour April 15, 2021, 2021.
25. J. M. Lee. Exploring walking behavior in the streets of New York City using hourly pedestrian count data. *Sustainability*, 12(19):7863, 2020.
26. C. V. Gál and N. Kántor. Modeling mean radiant temperature in outdoor spaces, a comparative numerical simulation and validation study. *Urban Climate*, 32:100571, 2020.
27. F. Lindberg, C.S.B. Grimmond, A. Gabey, B. Huang, C. W. Kent, T. Sun, N. E. Theeuwes, L. Järvi, H. C. Ward, I. Capel-Timms, Y. Chang, P. Jonsson, N. Krave, D. Liu, D. Meyer, K. F. G. Olofson, J. Tan, D. Wästberg, L. Xue, and Z. Zhang. Urban Multi-scale Environmental Predictor (UMEP): An integrated tool for city-based climate services. *Environmental Modelling & Software*, 99:70–87, 2018.
28. M. D. Dumas. Changes in temperature and temperature gradients in the French Northern Alps during the last century. *Theoretical and Applied Climatology*, 111(1-2):223–233, 2013.
29. Google. Google Satellite API, 2021. URL <https://mt1.google.com/vt/lyrs=s&x={x}&y={y}&z={z}>.
30. V. R. Melnikov, V. V. Krzhizhanovskaya, M. H. Lees, and P. M. A. Sloom. The impact of pace of life on pedestrian heat stress: A computational modelling approach. *Environmental Research*, 186:109397, 2020.
31. L. P. Ardigò, F. Saibene, and A. E. Minetti. The optimal locomotion on gradients: walking, running or cycling? *European Journal of Applied Physiology*, 90(3-4):365–371, 2003.
32. R. G. McMurray, J. Soares, C. J. Caspersen, and T. McCurdy. Examining variations of resting metabolic rate of adults: A public health perspective. *Medicine and science in sports and exercise*, 46(7):1352–1358, 2014.
33. A. H. Dewolf, Y. P. Ivanenko, F. Lacquaniti, and P. A. Willems. Pendular energy transduction within the step during human walking on slopes at different speeds. *PLOS ONE*, 12(10):e0186963, 2017.
34. A. E. Minetti, L. P. Ardigò, and F. Saibene. Mechanical determinants of gradient walking energetics in man. *The Journal of Physiology*, 472:725–735, 1993.
35. Federal Department of the Environment, Transport, Energy and Communications. *Nationales Personenverkehrsmodell*. Bern, 2019.

36. J. Molloy, C. Tchervenkov, T. Schatzmann, B. Schoeman, Beat Hintermann, and Kay W. Axhausen. MOBIS-COVID. *Arbeitsberichte Verkehrs- und Raumplanung*, 1621, 2021.
37. W. Meert and M. Verbeke. HMM with non-emitting states for map matching, 2018.
38. Federal Statistical Office. Schweizerische Gesundheitsbefragung, 2017.
39. W. Tobler. *Three presentations on geographical analysis and modeling. Non-isotropic geographic modeling: speculations on the geometry of Geography, and global spatial analysis*. National Center for Geographic Information and Analysis, Santa Barbara, 1993.